The influence of protic non-solvents present in the environment on structure formation of poly(γ-benzyl-L-glutamate) in organic solvents

Ioan Botiz,*[a] Nikolay Grozev,[a] Helmut Schlaad[b] and Günter Reiter*[a]

Received 3rd January 2008, Accepted 27th February 2008
First published as an Advance Article on the web 20th March 2008
DOI: 10.1039/b719946e

We present an experimental study of structure formation in a polypeptide hetero-arm star block copolymer solution, obtained by swelling thin films in chloroform solvent vapor to variable poly(γ-benzyl-L-glutamate) (PBLGlu) concentrations (c_p). Direct observation by optical microscopy allowed us to follow in real time nucleation and growth of ordered three-dimensional structures of ellipsoidal shape. At low c_p, growth stopped when c_p decreased below the solubility limit ($c_{critical}$) but additional structures were formed when c_p was rapidly increased to a higher value. Although water is not a solvent for this polymer, we demonstrate that water, even in trace amounts, is nonetheless considerably affecting solubility and consequently the process of structure formation. We have varied systematically the amount of water present in the environment. $c_{critical}$ changed from about 0.53 (dry, *i.e.* desiccated surrounding vapour phase) *via* $c_{critical} \approx 0.16$–$0.25$ for 30–50% humidity of the vapour phase to $c_{critical} \approx 0.03$ for a vapour phase at 100% humidity. We attribute this change in solubility to complexation of water molecules with PBLGlu α-helix, which increases the interfacial tension between the polymer and the solvent. We have tested our hypothesis by replacing water with other non-solvents for the polymer. Only protic non-solvents changed the solubility of PBLGlu in chloroform.

Introduction

Solubility characterizes the transition from a liquid disordered state to a solid ordered state in a solution. The solubility threshold describes the maximum amount of a compound that can be dissolved in a given volume of solvent at a specified temperature. Solubility is of fundamental importance in various scientific disciplines like chemistry, mineralogy, pharmacology or biology and applications in environmental, chemical engineering or material science ranging from biosorption, bioaccumulation, plant operation or pollution control to drug delivery with carbon nanotubes.[1,2] The solubility of a solute in a solvent depends on temperature[3–6] and increases with the vapor pressure of the surrounding gas phase.[7] The investigation of the influence of various parameters controlling solubility is thus of great importance in order to control or to manipulate the formation of solid (ordered) structures that may precipitate in solution.

The transition from a disordered to an ordered state represents a frequently encountered phenomenon.[8–11] As an example, one may think of crystallization, a first-order phase transition from a liquid to a solid state characterized by a well defined melting point. The melting point of organic solids can be reduced in the presence of a number of gases.[12,13] Related phenomena are freezing point depression or the increase of the boiling point (known as colligative properties).[14]

The dissolution of polymers in a solvent may depend on branching,[15] molecular weight degree of cross-linking[16] or polymer crystallinity[17] or crystal size.[18] In addition, solubility of polyelectrolytes is affected by pH,[5] ionic strength,[19] or polarity.[20] Polar substances tend to dissolve readily in polar solvents while non-polar substances do so in non-polar solvents. Hydrogen-bonding interactions between solute and solvent may increase solubility.

Ordering of polypeptides in thin solid films[21] and in solutions[22] has attracted our attention due to the variety of ordered structures observed which is attributed to various intra- and intermolecular specific or non-specific forces acting between polypeptide molecules and polypeptide and solvent molecules. Here, we attempt to explore how polypeptides interact to form nuclei that then grow into larger ordered structures, and how this process depends on polymer concentration and environmental conditions.

In a first-order phase transition, the appearance of a new phase always involves both, nucleation and the subsequent growth of these nuclei. Nucleation is the first step in the formation of a crystal involving a discontinuous change of an order parameter at the transition between the initial and the new phase.[23] The result of such an activated process, which relies on a rare statistical event of the formation of a critical nucleus,[24] is the appearance of nanoscopically small molecular clusters of the new crystalline phase.[25]

The driving force for nucleation and growth of crystals in solutions can be related to the supersaturation which can be defined as the difference $\Delta\mu$ between the chemical potentials of a molecule in solution and in the bulk of the crystal phase. Homogeneous nucleation is most likely to be the dominant process at high levels of supersaturation.[26] Supersaturation can also be expressed as:

[a]*Institut de Chimie des Surfaces et Interfaces CNRS-UHA/UPR 9069 15, rue Jean Starcky, BP 2488 F-68057, Mulhouse, France. E-mail: ioan.botiz@uha.fr; G.Reiter@uha.fr*
[b]*Max Planck Institute of Colloids and Interfaces, Colloid Chemistry, Research Campus Golm, Potsdam, 14424, Germany*

$$\Delta\mu = kT\ln(c_p/c_{critical}) \quad (1)$$

Here, k is the Boltzmann constant, T is the absolute temperature, c_p represents the concentration of polymer in solution and $c_{critical}$ is the critical concentration below which no nucleation and growth occurs. Thus, nucleation starts above $c_{critical}$ and depends on c_p in solution.

The probability of forming a nucleus is higher in solutions of higher concentration because the number of "available", dissolved molecules for nucleus formation is larger. In dilute solutions of low c_p, on the average the dissolved polymer molecules are further apart and the interactions between them are comparatively weak, making nucleation difficult or even impossible. Increasing c_p brings polymer molecules closer and closer. When c_p reaches the value of $c_{critical}$, the interaction forces between the polymer molecules become strong enough to bring a sufficient number of them together to form nuclei. Such nuclei then grow into ordered solid structures over large length scales.

In theory, the nucleation density N is directly related to supersaturation ratio $c_p/c_{critical}$ by the following relation:[26]

$$\ln N = \ln P - \frac{Q\beta\sigma^3\nu^2}{(kT)^3}\cdot\frac{1}{[\ln(c_p/c_{critical})]^2} \quad (2)$$

Here, P is an intercept (its exact value depends on the details of the theoretical model chosen) representing the maximum possible number of nuclei for $c_p = 1$, Q is characterizing the type of growth, σ represents the interfacial energy between nucleus and solution, β is a shape factor and ν represents the volume of the monomeric species. The above equation is a result of Nielsen's main assumptions:[27] the number of monomers in an aggregate or cluster at critical radius for nucleation was assumed to be constant and all nuclei have been generated by the time $t = t_1$ (time scale for nucleation).

In the present study we investigate the processes of nucleation and growth of ordered structures under different environmental conditions as a function of concentration in thin films of polypeptide solutions. By exposing thin solid films to solvent vapor, we are transforming them into solutions where we will study nucleation and growth of ordered three-dimensional structures. In particular, we will focus on the influence on polymer solubility of humidity or other protic non-solvents present in the surrounding air by systematically varying the amount of water or other protic non-solvents present in the environment.

Experimental

For our studies, we used poly(γ-benzyl-L-glutamate) (PBLGlu) polymers of various molecular weights and architectures, all showing qualitatively similar results. Thus, in the here presented results, we focused on the most complex polymer, an AB_n heteroarm star block copolymer, denoted PS_{63}–$(PBLGlu_{37})_8$, consisting of eight poly(γ-benzyl-L-glutamate) (PBLGlu = B) blocks in average, attached to the backbone of a single amorphous polystyrene (PS = A) block (see the chemical structure in Fig. 1a). A schematic representation of this polymer and of one possible arrangement of the helices in an ordered state are given in Fig. 1b and 1c, respectively. Details about the synthesis and the characterization of this polymer are given in the Appendix. This class of rod–coil "molecular chimeras"[22] takes the advantage of one block which can generate order on different levels based on its primary and secondary structure.[28–31] The α-helical secondary structure (18/5 helix with a diameter of 1.6 nm)[21,32–34] of PBLGlu is a result of intramolecular hydrogen bonding. This helical structure represents a rigid macrodipole, *i.e.* it has an overall dipole moment (3.5 Debye per repeat unit)[35] caused by the organization of the individual dipoles of the carbonyl groups of the peptide bond pointing along the helix axis.

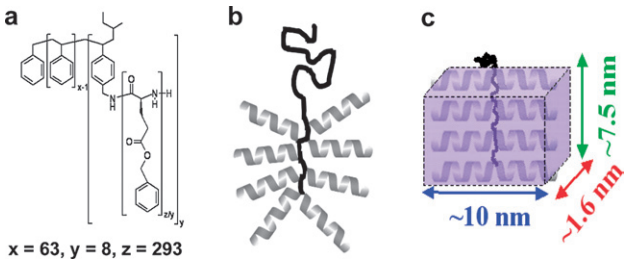

Fig. 1 a) Chemical structure; b) schematic representation of PS_{63}–$(PBLGlu_{37})_8$ heteroarm-star block copolymer; c) three-dimensional representation of a possible arrangement of the helical peptide block in the ordered state.

Thin solid films of PS_{63}–$(PBLGlu_{37})_8$ with an average thickness of few tens of nanometres (measured by ellipsometry) were obtained by spin-casting of chloroform ($CHCl_3$) polymer solutions onto hydrophilic UV/ozone-cleaned silicon wafers. Increasing molecular mobility by heating the polymers was not possible as the polymers degraded before melting. The morphology of none of these spin-coated solid films changed in time, even when heating the films to 200 °C for 60 min. Thus, these films were exposed to solvent vapor in order to increase the mobility of the polymer chains, which, in turn, enabled structure formation processes. After structure formation, the dry samples were characterized in detail by optical microscopy (OM) [Leitz, Metallux 3, Germany] and atomic force microscopy [Dimension 3000, Nanoscope III, Veeco, USA] in the tapping mode (TM-AFM).

Silicon substrates were used because of their excellent reflective properties which, coupled with an interference phenomenon due to light reflected at the film–air and substrate–film interfaces, gave us the possibility to use OM for our studies. In addition, we were using thin films because we could easily swell them until they became a "solution". More importantly, this approach also enabled us to study processes of structure formation in solutions in real time and direct space by OM. Another advantage of using thin films is related to the possibility that we could straightforwardly vary and evaluate directly the polymer concentration (c_p) by determining the thickness of the swollen films, deduced from the interference colors.

Interference colors were calibrated in order to obtain rather precise values of the (solution) film thickness. First, several films with different thicknesses (in steps of about 20 nm between 5 and 200 nm in thickness) were spin-coated from solutions of increasing polymer concentration. The thickness of each film was measured in the dry state by ellipsometry. In parallel, the interference color of each film was determined by OM. Consequently, we obtained a series of distinct interference colors

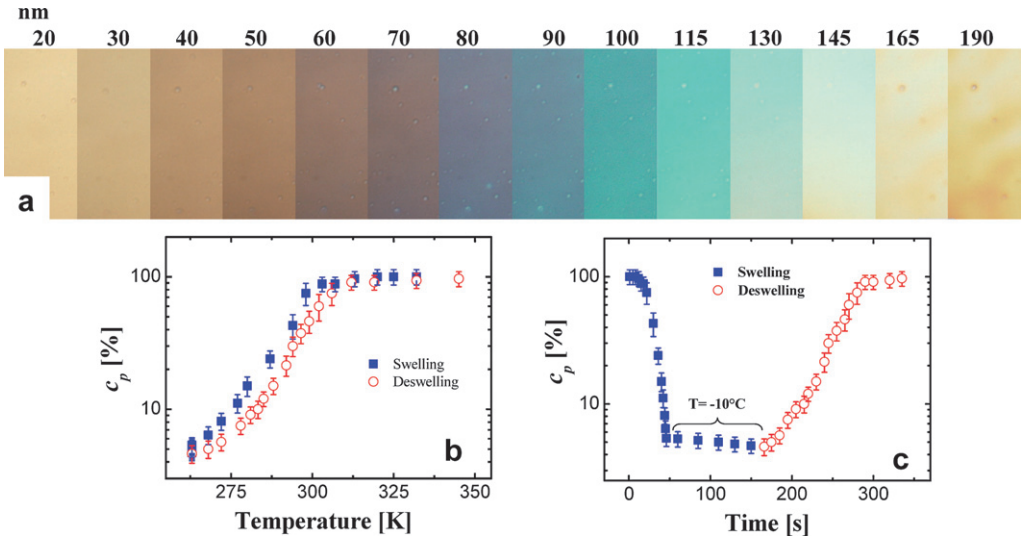

Fig. 2 Swelling and de-swelling of thin films: a) calibration series used in this study (color *versus* film thickness, ranging from 20 up to 190 nm); b) evolution of the polymer concentration during swelling and de-swelling as a function of film temperature; c) corresponding temporal evolution of the polymer concentration during swelling and de-swelling (using chloroform vapor).

together with the corresponding film thicknesses. The thickness of films having an interference color in between these calibrated colors was interpolated, allowing to continuously determine the thickness of a "film-solution" during swelling and de-swelling. The calibration films used are shown in Fig. 2a. Taking into account that the colors depend somewhat on the set-up of the optical microscope (light intensity, sensitivity of the CCD detector), the refractive index (which slightly depends on c_p), and the subjective judgment of the experimenter, we obtained an absolute thickness resolution of about 10 nm. However, relative changes during swelling/de-swelling and during structure formation could be observed with a higher precision of a few nanometres.

By exposing thin films to solvent vapor, the swelling of thin films could be done using two different approaches: either by condensation of solvent vapor onto the cooled film surface ("off-equilibrium" experiments) or by exposure of thin films to chloroform under conditions without any gradients in temperature (thermodynamic "equilibrium" experiments). Condensation is controlled by temperature to which the film surface was cooled below the temperature of the ambient solvent vapor phase.

It is important to emphasize that during both approaches, the polymer molecules were in contact with water molecules from the air. In order to obtain dry air conditions, we used phosphorus pentoxide (P_2O_5) as a desiccant. It absorbed water molecules from the ambient air very efficiently as the contact area between the P_2O_5 powder and air was large.

To expose thin solid films to solvent vapor, we used a home-built sample chamber. It contained two compartments connected *via* an opening that could be closed when needed. Using two compartments (one for solvent and one for the sample) allowed to cool or to heat between about −10 °C and 65 °C both the sample and the solvent independently by using separate Peltier heating/cooling stages for each compartment. The limited temperature range imposed by the Peltier elements did not allow us to use solvents with high boiling points and low volatility (for example dimethylformamide (DMF) with a boiling point of 153 °C). However, solvents such as $CHCl_3$ or tetrahydrofuran (THF) were well suited.

When performing "off-equilibrium" experiments, we sent solvent (heated to 50 °C in the solvent compartment) into the neighbouring compartment where the sample was initially kept at 35 °C. The walls of the sample compartment, however, were not heated. Thus, the sample chamber always stayed approximately at room temperature, with the exception of the sample stage it contained. After a few minutes, the sample was in equilibrium with solvent vapor at the temperature of the sample compartment. Under such conditions, not much solvent could be found in the film as its temperature was above the temperature of the vapor phase, which was mainly determined by the temperature of the walls of the sample chamber. Decreasing the sample temperature a few degrees below the temperature of the surrounding vapor phase led to solvent condensation onto the film and allowed for its swelling. We note that simultaneously with condensing solvent onto the films also a small amount of water from the surrounding air within the chamber was condensed onto the film if no precautions (P_2O_5) against humidity were taken.

We followed solvent condensation *via* the change of the interference colors of the film in real time and direct space by using an optical microscope. As the amount of polymer in the film stayed constant (this quantity is proportional to the thickness of the dry spin-coated film), a change in film thickness was directly related to the amount of solvent incorporated into the film, *i.e.* corresponded to swelling by solvent. From the interference colors we deduced the thickness (h) of the swollen film. The initial film thickness (h_0) was determined by ellipsometry. Accordingly, the polymer concentration c_p in the solution of the swollen film was determined by $c_p = h_0/h$. In Fig. 2b, we show a typical temperature dependence of c_p in the film during swelling/de-swelling, for a constant temperature of the solvent reservoir. The corresponding evolution in time is shown in Fig. 2c. Keeping the film at a constant and low temperature led to a slow but steady decrease of the c_p due to continuously condensing solvent

molecules (see Fig. 2c for the lowest c_p). Thus, for experiments of long durations, c_p was kept roughly constant by continuously increasing slightly the sample temperature. Analogous to swelling the film *via* solvent condensation, c_p could be augmented by increasing the sample temperature and thereby evaporating solvent from the film. We observed a pronounced hysteresis in $c_p(T)$. At a given temperature, c_p differed between the decreasing and the increasing temperature branch (see Fig. 2b). Finally, at a time chosen to stop the experiment, the sample was dried completely by simply heating the film to relatively high temperatures, for example to 65 °C.

In summary, we distinguish three stages during exposure of thin films to solvent vapor: 1) swelling of films up to (low) c_p; 2) controlled de-swelling by partial evaporation of the solvent from the swollen films; and finally 3) complete drying of films.

Results

We first present the results for the simpler situation where humidity was extracted from the surrounding air with the help of a desiccant. These results will then serve as a reference state for determining the influence of humidity on the solubility of polypeptides in good solvents.

In order to obtain high molecular mobility of polymers, we first swelled the films until c_p decreased to about 5%. At this concentration, the molecules were dispersed homogeneously and the molecular mobility was high. As the viscosity of the isotropic solution is comparatively low, surface tension was able to smoothen the surface of the film quickly within seconds (inhomogeneities observed by OM on spin-coated films disappeared). We took this smoothening process as a clear indication for having reached the isotropic phase. According to published works,[36,37] a transition between an isotropic and an adjacent liquid crystalline (LC) phase occurs at a threshold c_p of about 10–15%. Based on published data on related systems[22,25,37–49] the LC phase is supposed to be a cholesteric phase.

At c_p of about 5%, we did not observe any changes in time detectable by OM. The films stayed smooth for many hours. However, when we increased c_p to above 50%, we noticed that the films started to exhibit local changes in thickness (the corresponding heterogeneities on the film surface could be observed directly under the optical microscope), which we related to the formation of ordered structures within the film. At such increased c_p, the molecules got closer on the average and nuclei could be formed leading to the growth of ordered structures. This process is similar to undercooling a polymer melt, allowing thus for nucleation and growth of ordered solid structures. We cannot decide yet if these ordered structures grew from a homogeneous solution or from an already (pre)ordered LC phase. However, subsequently performed AFM measurements do not indicate any order of the phase surrounding the nucleated structures.

In Fig. 3, we present a typical example that demonstrates that OM allowed us to follow *in situ* both the exposure of films to solvent vapor, *i.e.* the formation of a solution film by solvent swelling, and the structure formation process. Fig. 3a shows the smooth, homogeneous surface of an initially 50 ± 2 nm thick film that had been already swollen in $CHCl_3$ vapor (using an "off-equilibrium" approach) up to a thickness of about

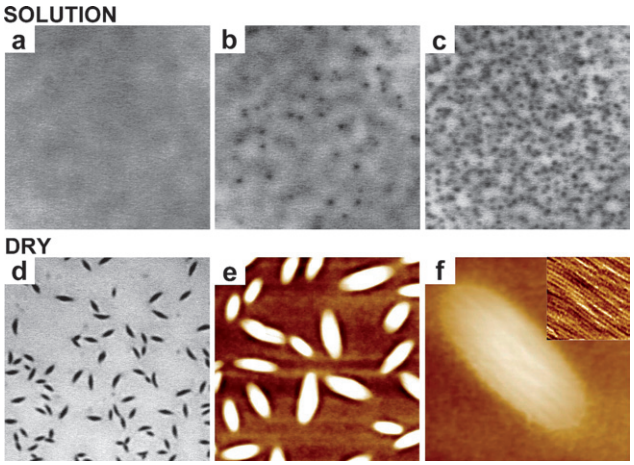

Fig. 3 Series of optical micrographs (a–d) and AFM topography (e, f) images showing the temporal evolution of a 50 ± 2 nm thick film at c_p = 53 ± 5%: a) after 20 minutes; b) after 25 minutes; c) after 30 minutes and (d–f) the final film morphology after total drying of the film. This film was spin-coated from chloroform solution and swollen under dry air conditions (P_2O_5) using chloroform vapor. The in-set in f) represents an AFM phase image zoomed into a region on top of the ellipsoidal structure. The size of the images is: 100 × 100 μm² (a, b, c); 35 × 35 μm² (d); 5 × 5 μm² (e), 0.8 × 0.8 μm² (f), respectively. The size of the in-set in f) is 250 × 250 nm².

1 micrometre and was then brought back to 95 ± 5 nm, *i.e.* to c_p of about 53 ± 5%.

After reaching a polymer concentration of 53 ± 5%, the surface stayed homogeneous for about 20 minutes (see Fig. 3a). After this time, isolated inhomogeneities started to appear randomly on the surface as observed directly under the optical microscope (see Fig. 3b). Of course, OM has its limitations in resolution (the lateral resolution in this case is about 1 micrometre) and the optical contrast is typically weak. This contrast is generated mainly by variations in film thickness and only weakly by the small differences in refractive index between the solution and the solid phase. Fortunately, at this concentration of c_p = 53 ± 5%, the growth process was slow enough to be followed in real time. In addition, the nucleation density was low enough so that individual objects were sufficiently separated and could be resolved by OM. Thus, structure formation could be clearly detected, starting after approximately 25 minutes at 53 ± 5% of polymer. After about 30 minutes, the surface was completely covered with isolated objects (Fig. 3c). It is worth mentioning that OM allowed us to verify that these structures existed already in solution and were not formed only at a later stage, for example during the drying of the film. After the rather rapid initial stage of their formation, these objects did not further increase significantly in size, even for prolonged times of up to one day. We attribute this stop in growth to the reduction of the concentration of the solution surrounding these objects below the critical concentration of supersaturation.

After 30 minutes at 53 ± 5% of polymer, the sample was rapidly dried and analyzed by OM and AFM. We could identify isolated, randomly distributed ellipsoidal structures embedded in a surrounding film of low degree of order, as shown in Fig. 3d–e. A detailed morphology of such an ellipsoidal three-dimensional

structure is shown in Fig. 3f. In the inset of this figure, we present the result of the phase-contrast of AFM, which clearly allows to detect parallel straight stripes on top of an ordered ellipsoidal structure. These stripes are spaced at an average characteristic distance of molecular dimension: 11 ± 3 nm (which is comparable to about two times the contour length of a $PBLGlu_{37}$ α-helix). Intermolecular hydrogen bonds may act normal to long axis of PBLGlu α-helices, which probably explains the existence of parallel straight stripes spaced at a molecular distance covering homogeneously the whole surface of the grown objects. Complementary "off-equilibrium" and "equilibrium" experiments (not shown in here) have been performed, which proved that the results obtained *via* the two approaches are equivalent.

In Fig. 4, we present the experimentally determined dependence of the number density $N(c_p)$ of ellipsoidal objects nucleated in thin films swollen in chloroform vapor to variable c_p (ranging from 53 up to 85% of polymer) under dry air conditions. At $c_p = 53 \pm 5\%$, ordered structures have been obtained as it is shown in Fig. 4a. As we can observe in Fig. 4b–e, the number of ordered ellipsoidal structures increased with c_p. At the same time, the size of ordered ellipsoidal structures decreased. Fig. 4f represents a summary of $N(c_p)$ for all experiments that we have performed under dry air conditions. N, the total number of structures per unit area, was determined by OM and/or AFM after complete drying of the films. N was found to increase with c_p (see Fig. 4f) as it is less difficult to form a nucleus at higher c_p when molecules are close to each other. However, when there are lots of nuclei per unit volume forming, then they will grow and rapidly meet each other (coalesce) due to the short distance between the nucleation sites. No further growth is possible afterwards. Thus, the average size of the structures will be small (see Fig. 4d–e). In order to have bigger structures, we decreased c_p till only few objects nucleated which then could grow to larger sizes

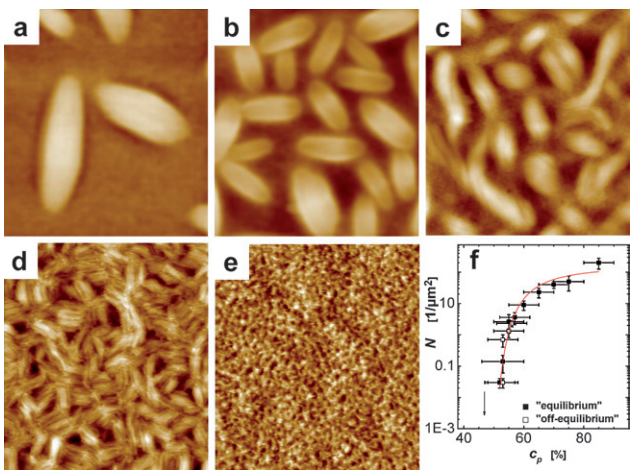

Fig. 4 Series of AFM topography images showing the morphology of dried 50 ± 3 nm thick films after having been swollen for about 0.5 to 2 hours at different c_p: a) 53%; b) 55%; c) 57% d) 65%; e) 85%. The dependence of the nucleation density N on c_p is shown in f). Thin films were spin-coated from chloroform solution and swollen under dry air conditions (P_2O_5) using chloroform vapor. Note that for a) and b) "off-equilibrium" type experiments, while for c), d) and e) "equilibrium" type experiments have been used, respectively. The size of all images is 2.5 × 2.5 µm².

(see Fig. 4a). Consequently, in order to be able to use optical microscopy as an observation tool, we concentrated our work on concentrations close to $c_{critical}$ where the formed structures could exceed the micrometre size. Interestingly, all films which were exposed at c_p lower than 53% showed neither inhomogeneities during exposure to chloroform vapor nor ordered structures after drying of the films detectable by OM or AFM. Thus, we conclude that the solubility limit in chloroform (or $c_{critical}$) was below 53%. An extrapolation of the $N(c_p)$ curve shown in Fig. 4f to 10^{-8} objects per µm² (one object per cm², *i.e.* one object/film surface) yielded $c_{critical} = 47 \pm 3\%$ (see the black vertical line in Fig. 4f). In order to obtain the error bars for this value of $c_{critical}$, we took into account the uncertainty in determining the polymer concentration $\Delta c_p = \pm 5\%$ for each point of the $N(c_p)$ curve. Two graphical extrapolations, using either the highest and lowest possible values given by Δc_p, to 10^{-8} objects per µm² were made, yielding $\Delta c_{critical} = \pm 3\%$.

We have also followed the ordering process in real time under ambient air conditions without P_2O_5 as desiccant to prevent the humidity in the surrounding gas-phase, performing both, "off-equilibrium" and "equilibrium" experiments in chloroform vapor. During the "off-equilibrium" film-swelling process, when condensing solvent vapor onto the film surface, some water molecules were also condensed and during the "equilibrium" experiments, thin films were also in contact with water molecules contained in surrounding gas-phase. Our results revealed that ordered ellipsoidal structures (the resulting morphology as detected by AFM did not change) could be obtained down to c_p as low as about 16–25%. Below c_p of 16–25%, no nucleation and growth of structures could be detected. This raises the question of why in ambient humid air structures could be formed at such low c_p? We have seen that under dry air conditions the concentration, below which structures could not nucleate and grow, was as high as 47%. Obviously, the only difference between both experiments is the presence of some water molecules in the surrounding gas phase, noting that water does not dissolve our polymer.

Apparently, humidity could influence $c_{critical}$. To rationally explore such a possibility, we have classified all our results obtained under ambient air conditions as a function of the humidity in our laboratory. We have observed that the series of results that was obtained in air of 30% humidity differed from the series under 50% humidity (see in Fig. 5 the right and left turned triangles, respectively). As we can observe in Fig. 5, the two series led to two different $c_{critical}$ values: about 25 ± 3% and 16 ± 2%, respectively, below which no structure formation was observed.

Already in 1984, Russo and Miller showed that a small amount of water, which can be easily absorbed even from the atmosphere under normal ambient conditions, seriously alters the phase behavior and morphology of the PBLGlu homopolymer solutions.[50] This observation is also relevant for our experiments presented here. When swelling our films in humid air, water molecules from the atmosphere obviously entered the polymer solution film. Based on our experiments we conclude that water, a non-solvent for our polymer system, facilitates ordering and structure formation even down to low concentrations.

In order to fully prove this statement, we have performed complementary experiments on films prepared at 100%

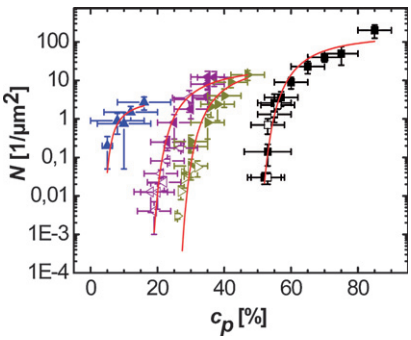

Fig. 5 Representation of nucleation density N *versus* polymer concentration c_p as determined from "off-equilibrium" (filled symbols) and "equilibrium" (empty symbols) experiments carried out: in dry air (■), at low humidity (▶), at high humidity (◀) and in water vapor saturated air (▲).

humidity. Under such conditions, a higher amount of water molecules was expected to condense on the film surface during the film-swelling process. Such conditions of water saturated air (100% humidity) were obtained by depositing a few droplets of water in the sample chamber before the film-swelling process was started. As the vapor pressure of chloroform was higher than that of water, we expected to have less water molecules than chloroform molecules in the surrounding gas-phase. Nonetheless, at 100% humidity, a significantly larger amount of water molecules condensed on the film surface during the swelling process compared to the case of ambient air conditions (30–50% humidity).

In the corresponding experiments, we exposed 25 ± 2 nm thick films to chloroform vapor under "off-equilibrium" conditions. The subsequent OM and AFM investigation performed after drying of the film revealed ellipsoidal ordered structures (not shown). Our results for various concentrations of the solution films studied are summarized in Fig. 5 (see the blue triangles). They prove that it was possible to form ellipsoidal ordered structures under 100% humidity conditions even at very low c_p of about 3–5%. We have experimentally determined (by extrapolation) a $c_{critical}$ of about 0.5 ± 0.4% below which no structure formation was observed. We would like to add that our approach for determining the concentration introduces a large uncertainty for very low values of c_p.

The full lines in Fig. 5 represent the best fits to the experimental data based on eqn (2). These fits contained three parameters: P, $C = Q\beta\sigma^3\nu^2/(kT)^3$ and $c_{critical}$. The fitted values of $c_{critical}$ were compared to the ones obtained by graphical extrapolation and are summarized in Table 1. As we can observe, the two sets of values were not differing much.

Table 1 Comparison of $c_{critical}$ values obtained both graphically (by extrapolation) and by fitting of eqn (2) to the data, respectively, for different humidity conditions

Humidity (%)	Extrapolated $c_{critical}$ (%)	Fitted $c_{critical}$ (%)
0	47 ± 3	44.2 ± 2.3
30	25 ± 3	21.3 ± 2
50	16 ± 2	13.3 ± 2
100	0.5 ± 0.4	2.22 ± 1

In summary, our results have shown that while the resulting morphology (ellipsoidal objects) did not depend on the humidity of the surrounding gas-phase, the solubility value $c_{critical}$ decreased significantly with an increase of humidity in the surrounding gas-phase.

Discussion

Although water is not a solvent for the PS_{63}–$(PBLGlu_{37})_8$ star block copolymer system, the experiments presented in this work have proved that water was nonetheless affecting the process of structure formation. We have varied systematically the amount of water present in the environment. Under dry air conditions (zero humidity), ellipsoidal ordered structures were formed only in rather concentrated polymer solutions ($c_{critical} \sim 44$%, see Table 1). At 30–50% humidity of the surrounding air, ellipsoidal ordered structures were already obtained at c_p as low as about 15% and in water-saturated air, ellipsoidal ordered structures were formed even at a c_p of about 3–5%.

All these results are based on systematic studies of $N(c_p)$, in accordance with eqn (2). Of course, in eqn (2) N represents a theoretical value and is introduced as the number of nucleated objects per unit volume in a homogeneous solution. At the beginning of the nucleation process, N is not constant but increases in time. In order to compare our experimental results with the theory of homogeneous nucleation, we have to calculate the total number of particles formed per unit volume during the whole nucleation period:

$$N = \int_0^\infty J\mathrm{d}t \qquad (3)$$

To perform this integration, we have to know the nucleation rate J, which is a time-dependent function. J depends also on c_p. Moreover, c_p depends on time because during the growth of the crystals the number of dissolved polymer molecules in the surrounding solution decreases.

In Fig. 6, we present normalized profiles of the nucleation rate J (a), the polymer concentration c_p (b) and the nucleation density N (c) as a function of time, scaled with respect to the induction period t_1 (characteristic time at which point c_p reaches the value of the critical concentration $c_{critical}$ for nucleation, *i.e.*, after t_1, nucleation is no longer possible). Due to the use of an approximate expression for c_p (given in ref. 27), which is valid only for short times, c_p shown in Fig. 6b (dotted line) decreases to zero. The nucleation rate J would only be constant if the concentration of the surrounding solution would stay constant (molecules forming the nucleated structures would be replaced by freshly added molecules). In thin films of finite volume containing a fixed number of molecules, we will always observe a decrease in nucleation rate (see Fig. 6a) because c_p decreases (see Fig. 6b). However, c_p can only decrease to $c_{critical}$. When $c_{critical}$ is reached also the growth of ordered ellipsoidal structures stops, limiting their size, *e.g.* in the above presented experiments to a size of a few micrometres.

Knowing c_p, we can deduce J and thus N, the number of nuclei per unit volume created after the time t_1. As we can observe in Fig. 6c, N becomes constant at long times and determines the total number of nuclei which can be formed. This number corresponds to the experimentally observable

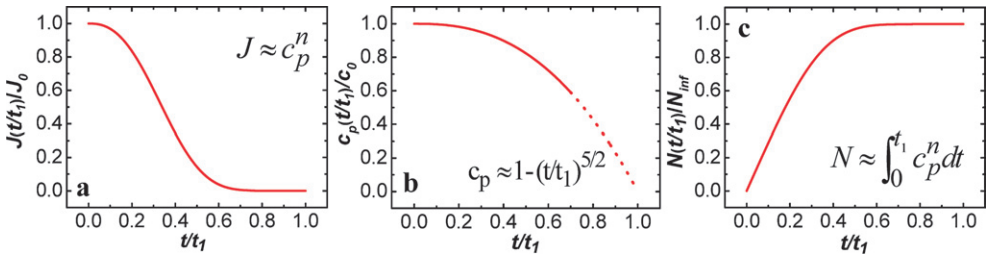

Fig. 6 Normalized profiles of J, c_p and N plotted as function of time t, scaled with respect to the induction period t_1. These curves resulted from the approximate expression for c_p given in ref. 27. Here c_0 represents the initial molecular concentration, J_0 is the initial nucleation rate corresponding to c_0, N_{inf} represents the nucleation density at infinite time and n was taken 10.

objects in polypeptide thin film solutions. Thus, it is justified to count the ellipsoidal ordered structures experimentally and to fit the resulting experimental $N(c_p)$ curves to the theoretical predictions (eqn (2)), yielding values for the three parameters: P, $Q\beta\sigma^3\nu^2/(kT)^3$ and $c_{critical}$. P is here the intercept. If one would represent log$N$ *versus* $(\log(c_p/c_{critical}))^{-2}$ one should obtain a straight line crossing the log$N$-axis at P. We have already shown (Table 1) that $c_{critical}$ varied with the humidity in the surrounding gas-phase: the higher the amount of humidity in the surrounding gas-phase was, the lower was the polymer solubility $c_{critical}$.

In Fig. 7a, we have plotted the fitted values for $Q^{1/3}\beta^{1/3}\sigma\nu^{2/3}/kT$, with only the interfacial tension σ between ordered structures and solution being a variable, as a function of humidity of the surrounding gas-phase. This presentation clearly showed that σ varied with humidity: the higher the amount of water, a non-solvent, in the surrounding gas-phase was, the higher was σ (see Fig. 7a). In Fig. 7b, we show that also $Q^{1/3}\beta^{1/3}\sigma\nu^{2/3}/kT$ and $c_{critical}$ are correlated. σ varied inversely with $c_{critical}$: the lower $c_{critical}$, the higher σ.

What could be the explanation for such dependence, knowing that water is not a solvent for γ-benzyl-L-glutamate because of the apolar benzyl groups? Also, water is not a solvent for PS and thus, the PS_{63}–$(PBLGlu_{37})_8$ polymer system cannot be dissolved in water. At the same time, PBLGlu offers several possible sites which can interact with water *via* hydrogen bonding interactions (for example the polar L-glutamate backbone and the polar ester group). To conclude, we deal with system which "does not like water but, which easily forms large scale ellipsoidal ordered structures in the presence of water".

We propose, as a tentative concept to explain the dependence of σ on humidity of the surrounding gas-phase, that protic non-solvent (water) molecules form a complex with PBLG *via*

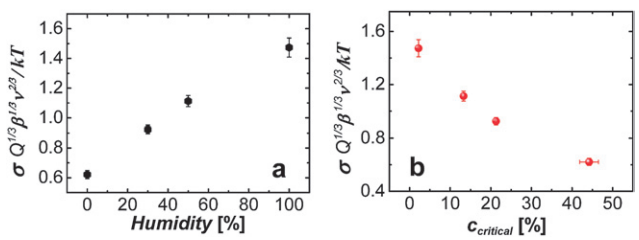

Fig. 7 Variation of interfacial tension σ between the solid ordered structures and solution: the interfacial tension σ increased with the increase of humidity in the surrounding gas-phase and with the decrease of polymer solubility $c_{critical}$.

hydrogen-bonding interactions and that this complex exhibited a lower solubility $c_{critical}$. Among the various possibilities for hydrogen bonding, the two hydrogen bonds of type C═O···H–O between the oxygen atom of the ester carbonyl group and hydrogen atom of water seem to be most favourable. The ester group is located at the exterior of the PBLGlu helix and not otherwise involved in hydrogen bonding. The secondary amide groups of the PBLGlu backbone, on the other hand, are involved in intramolecular hydrogen bonding,[51] stabilizing the α-helical conformation of PBLGlu, and are hidden inside the core of the helix. Some other type of hydrogen bonding interactions (for example C–H···O–H) can not be excluded but are considered to be less probable.

If this concept is valid, it means that also other non-solvents, with similar properties akin to water, should also be able to complex the PBLGlu and to modify its solubility. This concept also implies that non-solvents without these properties should not be able to complex the polymer. If these conclusions were proven, they would represent a strong support of our concept of polymer complexation.

In order to test these conclusions, we have performed three series of "off-equilibrium" experiments by exposing thin films to chloroform vapor mixed with a small amount of methanol, trifluoroacetic acid (TFA) and toluene molecules, respectively. Methanol and trifluoroacetic acid are "strongly hydrogen bonding" protic non-solvents that can form hydrogen bonds with the polymer. Toluene, although it is a good solvent for PS, does not dissolve PBLGlu (at room temperature). It is an aprotic "poorly hydrogen bonding"[52] non-solvent for PBLGlu and does not strongly interact with PBLGlu and does certainly not form hydrogen bonds.

Small amounts of methanol, TFA, or toluene molecules were added to the surrounding gas-phase by placing several droplets of these liquids in the sample chamber before performing the swelling of the film. The humidity of the air was avoided either by flushing the sample chamber with nitrogen before the start of the experiment (in the case of methanol, as methanol was absorbed by P_2O_5) or using P_2O_5 (in the case of TFA and toluene).

In Fig. 8 we have summarized the corresponding results. Systematic studies performed using methanol and toluene revealed that the morphology of the formed objects did not depend on the type of non-solvent we had used. With respect to results obtained in dry air, we observed that methanol and TFA did decrease $c_{critical}$, while toluene did not, most likely because it could not form hydrogen bonds. Accordingly, these

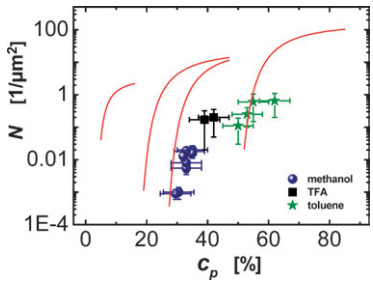

Fig. 8 Representation of nucleation density N *versus* c_p as determined from "off-equilibrium" experiments carried out by exposing thin films to chloroform vapor under dry air conditions in the presence of methanol (●), TFA (■) or toluene (★), respectively. Note that dry air conditions have been obtained either by using P_2O_5 (in the case of TFA and toluene) or by flushing the sample chamber with N_2 flow (in the case of methanol) before the film swelling. The red lines are the fits which were obtained according to eqn (2) for experiments performed under (from right to left): dry, less humid, more humid and highly humid air conditions, respectively (see Fig. 5).

results prove that complexation of PBLGlu by protic non-solvents *via* hydrogen-bonding interactions caused the decrease in solubility.

Conclusions

Optical microscopy allows us to directly observe in real time nucleation and growth of ordered polypeptide structures in thin solution films. The variation of the nucleation density (number of nuclei per area) with concentration could be determined by combining optical and atomic force microscopy. Interestingly, the nucleation density was sensitively affected by the humidity of the surrounding gas-phase. For example, while in dry air up to about 50% of polymer could be homogeneously dissolved in chloroform, only about 20–30% of polymer could be dissolved without formation of ordered structures. The influence of humidity may be expressed in terms of the critical concentration (solubility limit $c_{critical}$) below which no structures were formed. Increasing the humidity of the surrounding gas-phase led to a decrease of the value of the $c_{critical}$.

Independent of humidity, at concentrations slightly above $c_{critical}$, only few isolated objects could be nucleated, which then could only grow as long as the concentration of the surrounding solution stayed above $c_{critical}$, in accordance with theoretical predictions.

All the structures possessed an identical, anisotropic, ellipsoidal shape, which we relate to growth processing at different rates in the various directions. In addition, the surface of these structures exhibited straight parallel stripes of a width similar to the molecular dimension along normal to main chain axis. Based on these results, we tentatively interpret anisotropic structure formation as the result of differently strong specific directional interactions acting along the various axes of the molecules. Intermolecular hydrogen bonds may act normal to long axis of PBLGlu α-helices, which probably explains the existence of parallel straight stripes spaced at a molecular distance covering the whole surface of the grown objects.

The functional dependence of the number N of ordered objects per unit area on polymer concentration (c_p), in combination with theoretical considerations, allowed to determine a value for the interfacial tension σ between the polymer and the solution. The decrease in $c_{critical}$ with humidity can so be linked to an increase in σ. We believe that complexation between water and the PBLGlu chain, favored by hydrogen bonding interactions, is responsible for the decrease the "solubility" of the polymer, leading to ordering at even very low c_p. Furthermore, we demonstrated that also other protic solvents can cause a similar decrease in solubility. Consequently, the solubility of complex molecules like polypeptides, which contain sites of different polarity, hydrophilicity or hydrophobicity, not only depends on the quality of the solvent chosen but can also be varied by the presence of small amounts of a non-solvent of the whole molecules, which nonetheless can interact locally with specific sites on the molecule.

Appendix

Synthesis and characterization of the polymer

The polymer investigated is an AB_n heteroarm star block copolymer made polystyrene (PS = A) and poly(γ-benzyl-L-glutamate) (PBLGlu = B); the chemical structure is PS_{63}–$(PBLGlu_{37})_8$ with an average number of arms of $\bar{f} = \bar{n} + 1 = 9$. It was synthesized through polymerization of γ-benzyl-L-glutamate *N*-carboxyanhydride in *N*,*N*-dimethylformamide (DMF) solution at 40 °C initiated by a polystyrene$_{63}$-*block*-poly(4-aminomethyl-styrene)$_8$ (the subscripts denoting the average number of repeating units), as described earlier.[53]

^{1}H NMR analysis was applied to determine the chemical composition of the polymer (see spectrum in Fig. 9a), according to which the average number of BLGlu units is 297. Analytical ultracentrifugation results indicated a monomodal sedimentation-coefficient distribution of the polymer with a polydispersity index of PDI ∼ 1.5 (Fig. 9b). As evidenced by size-exclusion chromatography (SEC) in combination with FT-IR spectroscopy, the ensemble of chains is not uniform with respect to conformation or secondary structure (varying fractions of α-helix and

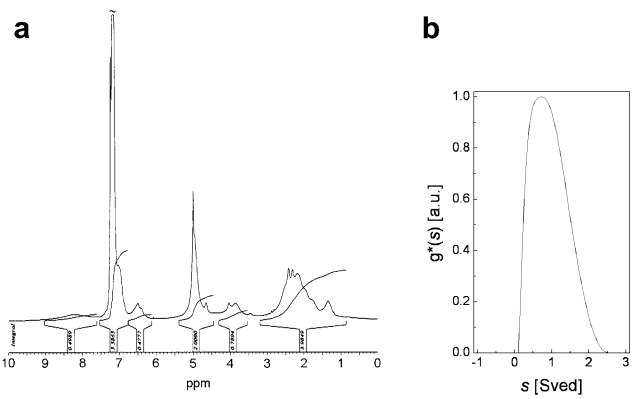

Fig. 9 Characterization of PS_{63}–$(PBLGlu_{37})_8$: a) ^{1}H NMR spectrum (400.1 MHz) of PS_{63}–$(PBLGlu_{37})_8$ in $CDCl_3$; b) sedimentation-coefficient distribution ($g^*(s)$) of PS_{63}–$(PBLGlu_{37})_8$, obtained in DMF at 40 °C and 50 K rpm (detector: Rayleigh interference).

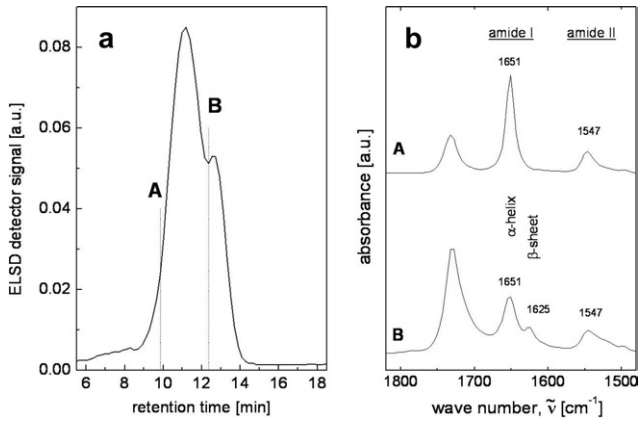

Fig. 10 Size-exclusion chromatogram (eluent: *N*,*N*-dimethylacetamide–isopropanol 90 : 10 (w/w), flow rate: 0.5 ml min^{-1}, temperature: 65 °C, stationary phase: 2 × 250 × 4.6 mm^2 RP-18, average particle size 7 μm, 1000 Å and 300 Å, detector: evaporative light scattering) (a) of PS_{63}–$(PBLGlu_{37})_8$ and FT-IR spectra (b) of the fractions eluting at 9.84 (A) and 12.35 minutes (B).

β-sheet; see Fig. 10); the estimated average fraction of BLGlu units in α-helical conformation is ~85%.

The number of arms of the polymer was estimated on the basis of intrinsic viscosity measurements. For a star polymer with regular arms under theta conditions, the relationship between the molecular contraction factor, *g*, and the number of arms, *f*, is given as

$$g = \frac{3f - 2}{f^2} \tag{4}$$

Furthermore, it is

$$g^{\varepsilon} = g' = \left(\frac{[\eta]_{star}}{[\eta]_{linear}}\right)_M \tag{5}$$

with $[\eta]_{star}$ and $[\eta]_{linear}$ as the intrinsic viscosities of the star-shaped and linear polymer molecules of the same molecular weight, *M*. Typical values for ε range from 0.5 (theta conditions) to 1.5.[54,55]

The intrinsic viscosities of AB_n and of a corresponding linear polymer ($AB:PS_{57}$-*b*-$PBLGlu_{233}$ with similar but not identical molecular weight as AB_n) in *N*,*N*-dimethylacetamide (+0.5 wt% LiBr) at 70 °C were determined as 127 ml g^{-1} and 599 ml g^{-1}, respectively; measurements were done with a VISKOTEK H502B coupled to a chromatographic system. With $g' \approx 0.22$ and $g \approx 0.05$–0.36 ($\varepsilon = 0.5$–1.5), the lower estimate for the number of arms of the heteroarm star block copolymer is calculated to be $f_{min} = 9$.

Acknowledgements

We are indebted and grateful to Hildegard Kukula (polymer synthesis), Antje Völkel (AUC measurement) and Jana Falkenhagen (BAM, Berlin; LC-FTIR measurements). We acknowledge financial support provided through the European Community's "Marie-Curie Actions" under contract MRTN-CT-2003-505027 [POLYAMPHI].

References

1 N. N. Nirmalakhandan and R. E. Speece, *Environ. Sci. Technol.*, 1989, **23**, 708.
2 A. Bianco, K. Kostarelos and M. Prato, *Curr. Opin. Chem. Biol.*, 2005, **9**, 674.
3 J. W. Hill, R. H. Petrucci, *General Chemistry*, Prentice Hall, 2nd edn, 1999.
4 C. D. Hodgman, in *Handbook of Chemistry and Physics*, Chemical Rubber Publishing Co., 27th edn, 1943.
5 S. P. Pinho, C. M. Silva and E. A. Macedo, *Ind. Eng. Chem. Res.*, 1994, **33**, 1341.
6 *Handbook of Chemistry and Physics*, ed. D. R. Lide, CRC Press, Cleveland, Ohio, USA, 88th edn, 2007.
7 T. R. Gilbert, R. V. Kirss, G. Davies, *Chemistry, the Science in Context*, W.W. Norton & Company Ltd. New York, 1st edn, 2003.
8 Y. Zhou, C. K. Hall and M. Karplus, *Phys. Rev. Lett.*, 1996, **77**, 2822.
9 A. K. Khandpur, S. Förster, F. S. Bates, I. W. Hamley, A. J. Ryan, W. Bras, K. Almdal and K. Mortensen, *Macromolecules*, 1995, **28**, 8796.
10 F. S. Bates, J. H. Rosedale and G. H. Fredrickson, *J. Chem. Phys.*, 1990, **92**, 6255.
11 K. E. Davis, W. B. Russel and W. J. Glantschnig, *Science*, 1989, **245**, 507.
12 A. Prins, *Vers. Akad. Wet. Amsterdam*, 1915, **17**, 1095.
13 S. G. Kazarian, N. Sakellarios and C. M. Gordon, *Chem. Commun.*, 2002, **12**, 1314.
14 F. C. Andrews, *Science*, 1976, **194**, 567.
15 S.-A. Chen and G.-W. Hwang, *J. Am. Chem. Soc.*, 1995, **117**, 10055.
16 W. W. Graessley, *J. Phys. Chem.*, 1964, **68**, 2258.
17 R. Pignatello, M. Ferro and G. Puglisi, *AAPS PharmSciTech.*, 2002, **3**, article 10.
18 R. M. Bennett, J. R. Lehr and D. J. Mccarty, *J. Clin. Invest.*, 1975, **56**, 1571.
19 C. J. Marzzacco, *J. Chem. Educ.*, 1998, **75**, 1628.
20 K. J. Williamson, *Macroscale and Microscale Organic Experiments*, Lexington, 2nd edn, 1994.
21 S. Ludwigs, G. Krausch, G. Reiter, M. Losik, M. Antonietti and H. Schlaad, *Macromolecules*, 2005, **38**, 7532.
22 H. Schlaad and M. Antonietti, *Eur. Phys. J. E*, 2003, **10**, 17.
23 D. W. Oxtoby, *J. Phys.: Condens. Matter*, 1992, **4**, 7627.
24 R. P. Sear, *J. Phys.: Condens. Matter*, 2007, **19**, 033101.
25 D. Kashchiev and G. M. van Rosmalen, *Cryst. Res. Technol.*, 2003, **38**, 555.
26 R. Mohanty, S. Bhandarkar and J. Estrin, *AIChE J.*, 1990, **36**, 1536.
27 A. E. Nielsen, *Krist. Tech.*, 1969, **4**, 17.
28 P. Papadopoulos, G. Floudas, H.-A. Klok, I. Schnell and T. Pakula, *Biomacromolecules*, 2004, **5**, 81.
29 B. Gallot, *Prog. Polym. Sci.*, 1996, **21**, 1035.
30 M. Lee, B.-K. Cho and W.-C. Zin, *Chem. Rev.*, 2001, **101**, 3869.
31 J. Rodríguez-Hernández and S. Lecommandoux, *J. Am. Chem. Soc.*, 2005, **127**, 2026.
32 H.-A. Klok, J. F. Langenwalter and S. Lecommandoux, *Macromolecules*, 2000, **33**, 7819.
33 E. A. Minich, A. P. Nowak, T. J. Deming and D. J. Pochan, *Polymer*, 2004, **45**, 1951.
34 M. Losik, S. Kubowicz, B. Smarsly and H. Schlaad, *Eur. Phys. J. E*, 2004, **15**, 407.
35 W. G. J. Hol, P. T. van Duijnen and H. J. C. Berendsen, *Nature*, 1979, **273**, 443.
36 R. Sakamoto, *Colloid Polym. Sci.*, 1984, **262**, 788.
37 E. L. Wee and W. G. Miller, *J. Phys. Chem.*, 1971, **75**, 1446.
38 P. J. Flory, *Proc. R. Soc. London, Ser. A*, 1956, **A234**, 60.
39 C. Robinson, *Trans. Faraday Soc.*, 1956, **52**, 571.
40 J. Watanabe, M. Goto and T. Nagase, *Macromolecules*, 1987, **20**, 298.
41 P. S. Russo and W. G. Miller, *Macromolecules*, 1983, **16**, 1690.
42 S.-J. He, C. Lee, S. P. Gido, S. M. Yu and D. A. Tirrell, *Macromolecules*, 1998, **31**, 9387.
43 J. Watanabe, K. Imai and I. Uematsu, *Polym. Bull.*, 1978, **1**, 67.
44 H. Toriumi, S. Minakuchi, Y. Uematsu and I. Uematsu, *Polym. J.*, 1980, **12**, 431.
45 I. Uematsu, *Adv. Polym. Sci.*, 1984, **59**, 37.
46 C. Robinson and J. C. Ward, *Nature*, 1957, **180**, 1183.
47 C. Robinson, J. C. Ward and R. B. Beevers, *Discuss. Faraday Soc.*, 1958, **25**, 29.

48 A. Hill and A. M. Donald, *Liq. Cryst.*, 1989, **6**, 93.
49 H. Block and C. P. Shaw, *Polymer*, 1992, **33**, 2459.
50 P. S. Russo and W. G. Miller, *Macromolecules*, 1984, **17**, 1324.
51 H. Schlaad, B. Smarsly and I. Below, *Macromolecules*, 2006, **39**, 4631.
52 J. Brandrup, E. H. Immergut, *Polymer Handbook*, 3rd Edition, 1989.
53 H. Kukula, H. Schlaad and K. Tauer, *Macromolecules*, 2002, **35**, 2538.
54 S. Mori, H. G. Barth, *Size exclusion chromatography*, Springer, Berlin, Heidelberg, 1999.
55 S. T. Balke, T. H. Mourey, D. R. Robello, T. A. Davis, A. Kraus and K. Skonieczny, *J. Appl. Polym. Sci.*, 2002, **85**, 552.